



Enhancing Molecular Studies with Multiwavelength Analytical Ultracentrifugation

Amy Henrickson, Beckman Coulter Life Sciences
Sameera Qureshi, Beckman Coulter Life Sciences

Introduction

In the realm of analytical ultracentrifugation (AUC) instruments, the integration of multiwavelength (MW) analysis has emerged as a groundbreaking approach for elucidating the interactions between multiple molecules with distinct absorbance profiles.⁷ The Optima AUC Analytical Ultracentrifuge from Beckman Coulter Life Sciences, equipped with Rayleigh interference optics and multiwavelength-capable UV/visible absorption optics (collectively known as “Beckman optics”), epitomizes this technological advancement.⁶

This white paper delves into the principles and applications of multiwavelength analytical ultracentrifugation (MW-AUC) as an advanced method for studying biopolymer interactions under physiological conditions. Through a series of research experiments, we illustrate the efficacy of the Optima AUC in characterizing molecular interactions across various biological systems, including enzyme activity, viral vectors, protein-DNA interactions, biopolymer mixtures and lipid nanoparticles.

MW-AUC enables the study of biopolymer interactions in a physiological environment, where factors such as ionic strength, pH and redox potential can be precisely controlled.⁶ This technique measures samples while separating them using centrifugal force, allowing for high-resolution characterization of the different analytes in the solution. MW-AUC is particularly beneficial when the solution contains analytes with distinct absorbance spectra. By collecting data at multiple wavelengths, analytes can be differentiated based on variations in their hydrodynamic properties and absorbance characteristics. If the pure spectra of the individual analytes are known, the MW-AUC data can be decomposed into the pure spectra. This allows for the determination of stoichiometry and molar ratio for each analyte in solution.⁶

MW-AUC has advanced the analysis of various interacting systems, including protein-DNA,^{2,3} protein-RNA,⁴ biopolymers,⁵ heme proteins and amyloid- β peptide interactions,⁶ as well as the characterization of AAVs.^{1,7,8,9} Its capability to determine DNA insert length and wavelength-specific correction factors for different insert sizes has been demonstrated.⁹ Below, we present a few research experiments that were carried out using the Optima AUC and discuss how multiwavelength experiments helped scientists to further their research.

I. Biopolymer mixtures and interactions

To highlight the overall utility of MW-AUC, Henrickson et al.¹⁴ highlights two different examples. In the first, they look at an oilseed protein extract where the spectral properties of each analyte in solution are unknown, and in the second case, they look at a mixture of three proteins, where the pure spectral signature of each protein is known. In the oilseed protein extract, they employed MW-AUC to study and identify the components of the extract. The extract contained water-soluble polyphenols (315 nm absorbance peak) and proteins of unknown size. They wanted to determine if the polyphenols were bound to the proteins in the solution or remained free in the solution. MW-AUC revealed that most polyphenols sedimented at -0.5 – 1.0 S, while the primary protein (12.5 S) remained intact with no polyphenol interaction, whereas a smaller protein fraction (<2 S) suggested degradation with possible polyphenol binding. This study highlights that even if an optical deconvolution cannot be performed because the pure basis spectra are unknown, MW-AUC can still help to elucidate the answer by highlighting the spectral difference at each sedimentation coefficient.

II. Protein-DNA interactions

Ahmed et al.¹³ used AUC to investigate the interaction between DNA and ComEA, a critical protein in bacterial transformation. During transformation, DNA uptake into the periplasm is facilitated by type IV pili, which bind and retract DNA, while ComEA, a highly conserved DNA-binding protein, functions as a Brownian ratchet, driving the translocation of transforming DNA into the periplasm. They used AUC and X-ray crystallography to help elucidate the function of one domain on ComEA and used MW-AUC to investigate the interaction between DNA and the ComEA DNA-binding domain.

X-ray crystallography found that the unknown domain on ComEA appeared to be involved in the oligomerization formation of the proteins. AUC was used to confirm that this oligomerization occurred in solution and determine if it was reversible, and the results confirmed a monomer-dimer equilibrium with a K_D of 33.8 μM . Thus, the domain was called the oligomerization domain (OD). It was speculated that this OD also played an important role in ComEA binding to DNA. To test this, a mutant, ComEA-A108Y, was created, which prevents the oligomerization. Using MW-AUC, the researchers could confirm the total number of ComEA proteins binding to the DNA and identified that almost twice as many ComEA wild-type proteins could bind the DNA compared to ComEA-A108Y. The utility of the ComEA oligomerization process appears to facilitate the efficient and cooperative packing of ComEA on DNA, which is crucial for its function in bacterial transformation.

Horne et al.¹⁵ investigated the interactions between NanR dimers and between NanR and DNA. NanR, a transcription repressor, regulates sialic acid metabolism in *Escherichia coli*. Sialic acid coats human cell surfaces and serves as a nutrient source for both pathogenic and commensal bacteria. Their study demonstrated, using cryo-electron microscopy and MW-AUC, that three NanR dimers cooperatively and with high affinity bind to a (GGTATA)₃ repeat operator, providing a molecular basis for the regulation of bacterial sialic acid metabolism.

The researchers titrated NanR against the DNA repeat operator and measured the different titrations using MW-AUC recording scans within the 220-300 nm range at 2 nm increments. They then deconvoluted the sedimentation signal into the individual protein and DNA spectral signals, and could identify the NanR and DNA peaks co-migrating, indicating an interaction. At low NanR concentrations, a free DNA peak is also present (Fig. 1b), and as the NanR concentration was increased, the free DNA decreased. At the highest concentration, a free NanR peak appears, indicating saturation of the DNA (Fig. 1e). Due to the optical deconvolution, the researchers could also determine the number of NanR binding to the DNA at each titration, with a final molar ratio of NanR to DNA of 6.44:1, consistent with three NanR-dimer binding to the DNA. This study provided molecular insights into the regulatory mechanism governing bacterial sialic acid metabolism.

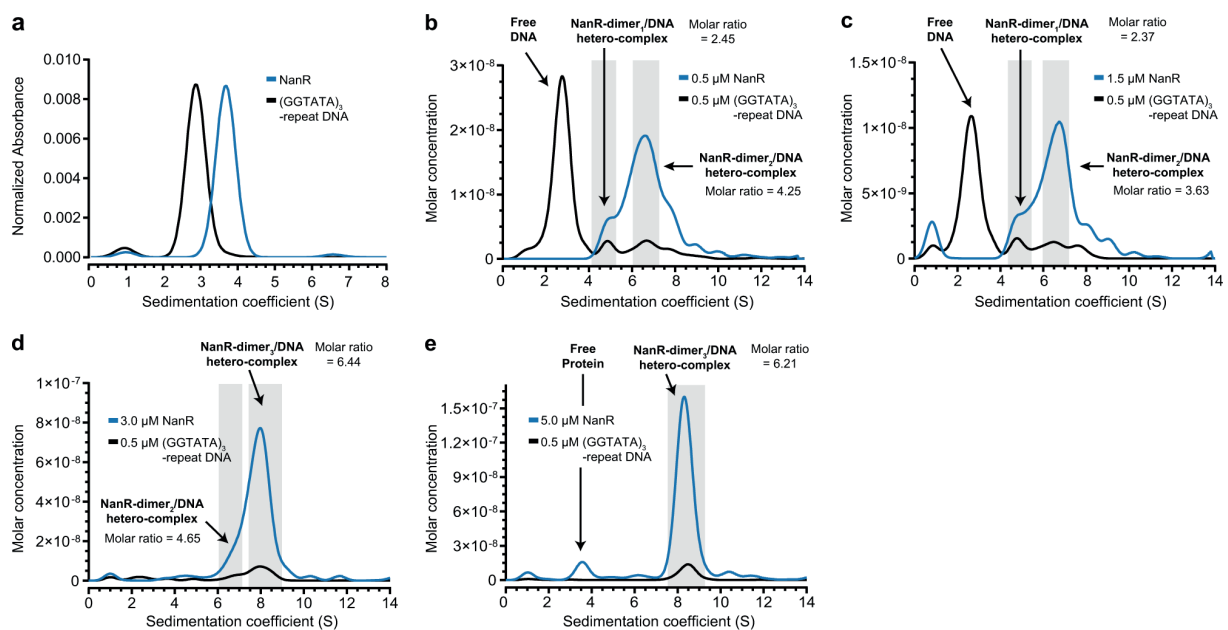


Figure 1. a: Sedimentation coefficient distributions of the NanR (blue) and the (GGTATA)₃-repeat DNA operator (black) controls, measured individually at 280 and 260nm, respectively. **b-e:** Deconvoluted sedimentation coefficient distributions resulting from the titration of NanR into (GGTATA)₃-repeat DNA (0.5 μM): 0.5 μM NanR (b), 1.5 μM NanR (c), 3.0 μM NanR (d), and 5.0 μM NanR (e). A shift in the sedimentation coefficient is observed with increasing NanR concentration, consistent with hetero-complex formation. The molar ratio of the integrated peaks (shaded in gray) and the oligomeric state of each hetero-complex is shown. The presence of excess protein free of any co-migrating DNA in e indicates that hetero-complex formation has reached saturation. All plots are presented as $g(s)$ distributions with the molar concentration for each interacting partner (protein and DNA) plotted on the y-axis.

This figure is reused under <https://creativecommons.org/licenses/by/4.0/> and has not been altered.

III. Viral vectors and MW-AUC

AUC has established itself as the gold standard method for adeno-associated virus (AAV) characterization, as it can characterize and quantify the different loading states of the viral particles as well as contaminants, including overfilled particles, aggregates and degradants. **Maruno et al.**¹² present an effective methodology for size distribution analysis and AAV vector loading states. This precise assessment is essential, as product-related impurities—including empty particles (EPs), intermediate particles (IPs) and aggregates—may reduce therapeutic efficacy and exacerbate undesirable immune responses. Using band sedimentation analytical ultracentrifugation (BS-AUC) with multiwavelength detection on the Optima AUC (Beckman Coulter Life Sciences), this approach enables precise separation of full particles (FPs), EPs, and IPs using a small amount of samples. The total peak area of the sedimentation coefficient distribution obtained from BS-AUC analysis corresponded with absorbance measurements determined via ultraviolet-visible (UV-Vis) absorption spectroscopy.

AAV loading state identification was achieved in MW-BS-AUC by analyzing the wavelength dependence of the $c(s)$ peak area, which corresponded to the spectral profile of each component. Additionally, minor peak identification was performed with greater precision and reliability using multiwavelength sedimentation velocity analytical ultracentrifugation (MW-SV-AUC). These approaches serve as a powerful analytical tool for AAV vector production process development, as well as for batch-to-batch and lot-to-lot quality assessments of AAV drug substances.

Henrickson et al.⁷ present MW-AUC as a highly accurate method for the characterization and quantification of AAV samples. The results were compared with dual-wavelength AUC, transmission electron microscopy, and mass photometry. Unlike dual-wavelength AUC, MW-AUC provides precise quantification of AAV capsid ratios and enables the identification of contaminants. In contrast to transmission electron microscopy, MW-AUC also detects and quantifies partially filled capsids. Furthermore, unlike mass photometry, MW-AUC yields first-principle results. This study highlights the enhanced analytical capabilities of MW-AUC, emphasizing the utility of recently integrated UltraScan programs and reaffirming AUC as the gold standard for viral vector analysis.

Richter et al.⁸ demonstrated the capability of MW-AUC to determine DNA insert length and derive wavelength-specific correction factors for varying insert sizes. The study compared biophysical methods for assessing the purity and DNA content of viral capsids across five AAV serotypes using multiwavelength detection at 230 nm, 260 nm and 280 nm. MW-AUC was employed to quantify species content and derive wavelength-specific correction factors for respective insert sizes.

At each detection wavelength—230 nm, 260 nm, 280 nm, and Rayleigh interference—empty, filled, and partially filled capsids were identified. In mixed populations analyzed using multiwavelength approaches, the measured contents varied by wavelength due to differences in extinction coefficients between empty and filled capsids. The results were further validated through comparisons with multiple orthogonal characterization methods, which produced consistent findings on empty and filled capsid content. While anion-exchange chromatography (AEX) and UV spectroscopy can quantify empty and filled AAVs, only SV-AUC successfully detected low levels of partially filled capsids.

The study demonstrated that modeling and confirming response factors for native AAVs with differently sized DNA constructs is now feasible due to the high resolution of SV-AUC. Additionally, SV-AUC enables precise determination of specific absorbance ratios, response factors and extinction coefficients for each capsid type, establishing it as the highest-resolution technique among those evaluated.

Conclusion

The application of MW-AUC using the Optima AUC from Beckman Coulter Life Sciences has significantly advanced our understanding of complex molecular interactions. The research examples presented herein underscore the versatility and precision of MW-AUC in various scientific inquiries, from enzyme regulation and viral vector characterization to protein-DNA binding dynamics and the analysis of biopolymer mixtures. The integration of MW-AUC into analytical workflows not only enhances the accuracy of molecular studies but also reaffirms its status as an indispensable tool in the field of life sciences, offering unparalleled analytical capabilities and contributing to the progression of molecular biology, virology and biochemistry.

References

1. Maruno T, Usami K, Ishii K, Torisu T, Uchiyama S. Comprehensive Size Distribution and Composition Analysis of Adeno-Associated Virus Vector by Multiwavelength Sedimentation Velocity Analytical Ultracentrifugation. *J Pharm Sci.* 2021 Oct;110(10):3375–3384. PMID: 34186069
2. Ahmed I, Hahn J, Henrickson A, Khaja FT, Demeler B, Dubnau D, Neiditch MB. Structure-function studies reveal ComEA contains an oligomerization domain essential for transformation in gram-positive bacteria. *Nat Commun.* 2022 Dec 13;13(1):7724. PMID: PMC9747964
3. Horne CR, Venugopal H, Panjikar S, Wood DM, Henrickson A, Brookes E, North RA, Murphy JM, Friemann R, Griffin MDW, Ramm G, Demeler B, Dobson RCJ. Mechanism of NanR gene repression and allosteric induction of bacterial sialic acid metabolism. *Nat Commun.* 2021 Mar 31;12(1):1988.
4. Zhang J, Pearson JZ, Gorbet GE, Cölfen H, Germann MW, Brinton MA, Demeler B. Spectral and Hydrodynamic Analysis of West Nile Virus RNA-Protein Interactions by Multiwavelength Sedimentation Velocity in the Analytical Ultracentrifuge. *Anal Chem.* 2017 Jan 3;89(1):862–870. PMID: PMC5505516
5. Johnson CN, Gorbet GE, Ramsower H, Urquidi J, Brancalion L, Demeler B. Multi-wavelength analytical ultracentrifugation of human serum albumin complexed with porphyrin. *Eur Biophys J.* 2018 Oct;47(7):789–797. PMID: PMC6158097
6. Henrickson A, Gorbet GE, Savelyev A, Kim M, Hargreaves J, Schultz SK, Kothe U, Demeler B. Multi-wavelength analytical ultracentrifugation of biopolymer mixtures and interactions. *Anal Biochem.* 2022 Sep 1;652:114728. PMID: PMC10276540.
7. Henrickson A, Ding X, Seal AG, Qu Z, Tomlinson L, Forsey J, Gradinaru V, Oka K and Demeler B. Characterization and quantification of adeno-associated virus capsid-loading states by multi-wavelength analytical ultracentrifugation with UltraScan. *Nanomedicine (Lond).* 2023;18(22):1519-1534. doi: 10.2217/nmm-2023-0156. Epub 2023 Oct 25.
8. Richter K, Wurm C, Strasser K, Bauer J, Bakou M, VerHeul R, Sternisha S, Hawe A, Salomon M, Menzen T, Bhattacharya A. Purity and DNA content of AAV capsids assessed by analytical ultracentrifugation and orthogonal biophysical techniques. *Eur J Pharm Biopharm.* 2023;189:68-83. doi:10.1016/j.ejpb.2023.05.011.
9. Bepperling A, Best J. Comparison of three AUC techniques for the determination of the loading status and capsid titer of AAVs. *Eur Biophys J.* 2023 Jul;52(4-5):401-413. doi: 10.1007/s00249-023-01661-0. Epub 2023 May 28. PMID: 37245172. doi: 10.1007/s00249-023-01661-0.
10. Henrickson A, Kulkarni JA, Zaifman J, Gorbet GE, Cullis PR, Demeler B. Density Matching Multi-wavelength Analytical Ultracentrifugation to Measure Drug Loading of Lipid Nanoparticle Formulations. *ACS Nano.* 2021 Mar 23;15(3):5068–76.
11. Potter JR, Rivera S, Young PG, Patterson DC, Namitz KE, Yennawar N, Kincaid JR, Liu Y, Weinert EE. Heme pocket modulates protein conformation and diguanylate cyclase activity of a tetrameric globin coupled sensor. *Journal of Inorganic Biochemistry*, 258, 2024, 112638, ISSN 0162-0134, <https://doi.org/10.1016/j.jinorgbio.2024.112638>.
12. Maruno T, Ishii K, Torisu T, Uchiyama S. Size Distribution Analysis of the Adeno-Associated Virus Vector by the c(s) Analysis of Band Sedimentation Analytical Ultracentrifugation with Multiwavelength Detection. *Journal of Pharmaceutical Sciences*, 112(4), 2023, 937-946. <https://doi.org/10.1016/j.xphs.2022.10.023>.
13. Ahmed I, Hahn J, Henrickson A, et al. Structure-function studies reveal ComEA contains an oligomerization domain essential for transformation in gram-positive bacteria. *Nat Commun* 13, 7724 (2022). <https://doi.org/10.1038/s41467-022-35129-0>.
14. Henrickson A, Gorbet GE, Savelyev A, Kim M, Hargreaves J, Schultz SK, Kothe U, Demeler B. Multi-wavelength analytical ultracentrifugation of biopolymer mixtures and interactions. *Analytical Biochemistry*, 652, 2022. <https://doi.org/10.1016/j.ab.2022.114728>.
15. Horne CR, Venugopal H, Panjikar S, et al. Mechanism of NanR gene repression and allosteric induction of bacterial sialic acid metabolism. *Nat Commun* 12, 1988 (2021). <https://doi.org/10.1038/s41467-021-22253-6>.
16. Henrickson A, Kulkarni JA, Zaifman J, Gorbet GE, Cullis PR, Demeler B. Density Matching Multi-wavelength Analytical Ultracentrifugation to Measure Drug Loading of Lipid Nanoparticle Formulations. *ACS Nano.* 2021 Mar 23;15(3):5068–76.
17. Mehn D, Iavicoli P, Cabaleiro N, Borgos SE, Caputo F, Geiss O, et al. Analytical ultracentrifugation for analysis of doxorubicin loaded liposomes. *Int J Pharm.* 2017 May 15;523(1):320–6.